



DLC-Coated Thermoplastics: Tribological Analyses under Lubricated Rolling-Sliding Conditions

S. Reitschuster¹ · E. Maier¹ · T. Lohner¹ · K. Stahl¹ · K. Bobzin² · C. Kalscheuer² · M. Thieux² · P. Sperka³ · M. Hartl³

Received: 20 July 2022 / Accepted: 2 October 2022 / Published online: 31 October 2022
© The Author(s) 2022

Abstract

The goal of this work is to evaluate the potential of diamond-like carbon (DLC) coatings on thermoplastic polymers for friction and wear reduction in highly stressed rolling–sliding contacts. Therefore, hydrogen-containing DLC coatings were deposited on the polymer surface by a low-temperature high power pulsed magnetron sputtering (HPPMS) physical vapor deposition (PVD) process. The rolling-sliding contact between coated polyamide 66 (PA66) or coated polyether ether ketone (PEEK) against case-hardened steel 16MnCr5 is investigated in a twin-disk tribometer at normal loads up to $F_N = 1,000$ N, sum velocities between $1 \text{ m/s} \leq v_{\Sigma} \leq 16 \text{ m/s}$ and slip ratios up to $s = 50\%$. Results show a friction reduction with the application of DLC on the considered polymers compared to uncoated polymers under specific lubrication conditions. High solid losses caused by the polymer's internal damping properties dominate the temperature behavior of the polymer, even when coated with DLC. Regarding the wear behavior, DLC coatings show potential especially under severe mixed lubrication conditions with high-solid load portion and sliding. The knowledge gained about coated polymers can be used to improve the overall tribological performance in terms of friction and wear of thermoplastic machine elements like gears.

Keywords DLC coating · Polymers · Lubrication · Friction · Temperature · Elastohydrodynamics

1 Introduction

The well-known advantages of thermoplastic polymers such as cost-efficient production and low density, compete with moderate strength and strong temperature-dependent material behavior [1, 2]. Particularly under dry conditions, severe wear can limit the lifetime of thermoplastic machine elements like gears. Therefore, in applications with high power transmission, oil lubrication is used to reduce wear and bulk temperature [3, 4]. The combination of high loads and associated very low material stiffness (high elastic deformations

resp. mechanical compliance) of polymers forms a (thermo-) elastohydrodynamically lubricated (TEHL) contact [5, 6]. As a result, convex contact pairings between polymer and steel like in a gearing show a pronounced contact conformity [7]. The large deformation of the contact region results in low hydrodynamic pressure. Significant pressure-induced increase in the lubricant viscosity is therefore not present, which is also reflected in the frictional behavior [7, 8].

As shown in [8], interfacial friction in polymer/steel contacts is low and depends largely on the surface characteristics. Furthermore, experimental investigations on a twin-disk tribometer and numerical calculations demonstrate that very low coefficients of friction in the range of superlubricity are possible, even in the mixed lubrication regime [8, 9]. Friction leads to increased temperatures in TEHL contacts. Besides heat sources from the shearing and compression of the lubricant as interfacial friction, some thermoplastic polymers also show solid losses. Even at pure rolling conditions, a bulk temperature increase is observed, indicating that heat generated by interfacial friction is subordinate [8]. Solid losses can originate from the viscoelastic material behavior and show a strong load and frequency dependency

✉ S. Reitschuster
stefan.reitschuster@tum.de

¹ School of Engineering & Design, Department of Mechanical Engineering, Technical University Munich, Gear Research Center (FZG), Boltzmannstraße 15, 85748 Garching near Munich, Germany

² Surface Engineering Institute (IOT), RWTH Aachen University, Kackertstraße 15, 52072 Aachen, Germany

³ Brno University of Technology (BUT), Technická 2896/2, 616 69 Brno, Czech Republic

that varies for each material. For example, high performance polyether ether ketone (PEEK) shows much lower solid losses under same operating conditions compared to polyamide (PA) [8]. Nevertheless, it should be noted that bulk temperatures and contact temperatures differ due to the low thermal diffusivity of polymers. This can lead to an accumulation of detrimental contact heat on the polymer surface [7]. In general, owing to the strong temperature dependency and the limited operating temperature range, the temperatures occurring in the polymer contact are important. If temperatures are too high, premature failure can occur far below the expected load limit.

The application of diamond-like carbon coatings (DLC) can improve the tribological performance of polymer components in terms of friction and wear. These coatings composed of graphitic sp^2 bindings and diamond-like sp^3 bindings are established on steel-based automotive components like tappets, piston, piston rings and camshafts since the early 2000s [10]. Nevertheless, transferring the deposition of the DLC coating systems from steel to polymer substrates is a major challenge. This is due to the chemical structure of the polymer substrate material and its incompatibility with metallic interlayers, since DLC coatings are primarily developed for deposition on metals. In addition, the effort for pre-treatment by means of grinding, polishing and etching of polymers is significantly increased compared to metallic materials but mandatory to ensure a sufficient adhesion between coating and substrate material. Lugscheider et al. [11] showed, that the adhesion between PVD coating and polymer substrate is improved by using combined pulsed magnetron sputtering compared to direct current (dc) or pulsed sputter process solely. Moreover, the coating properties have to be adjusted in accordance with soft polymer substrates, whereas hardened steels possess a sufficient load carrying capacity for the DLC coatings. There is a large variety of studies concerning the application of DLC on elastomers improving the friction and wear behavior, which is shown in the review of Martinez-Martinez and De Hosson [12]. In the field of endoprosthetics for artificial knee and hip joints, a multitude of studies describe the positive influence of DLC on the wear behavior of thermoplastics such as polyethylene in direct comparison with uncoated references, e. g. Rothhammer et al. [13], Puertolas et al. [14] and Onate et al. [15]. In contrast thereto, less studies are conducted with regard to the application of DLC on high performance thermoplastic materials such PEEK and PA66.

Kaczorowski et al. [16] analyzed DLC-coated PEEK against zirconium oxide under fluid-free conditions, which led to reduced friction and wear compared to uncoated surface modified PEEK at an initial Hertzian pressure $p_H = 117$ MPa. Furthermore, the adhesion between DLC and PEEK can be improved by N_2 etching instead of O_2 etching before deposition of the DLC coating. A friction

and wear reduction was also measured by Kapinski et al. [14] by testing DLC coated PA66 under dry lubrication against uncoated 100Cr6 at an initial Hertzian pressure $p_H = 160$ MPa. Analyses of DLC coated polymers under boundary and mixed friction at an initial Hertzian pressure $p_H = 345$ MPa prove, that besides a friction and wear reduction a chemical interaction with lubricant and additive is prevented [17].

Analytical and numerical calculations of Elsharkawy et al. [18] and Ziegltrum et al. [7] on the TEHL contact with DLC coated polymers against uncoated steel specimens demonstrate that the influence of the coating on the mechanical properties such as polymer stiffness and thus on hydrodynamic pressure and lubricant film thickness in the contact is low. In contrast to this, the thermophysical properties of DLC affect the contact temperature distribution also for very thin coatings. Due to a higher thermal diffusivity of DLC compared to polymers, the heat removal in the contact is more pronounced, resulting in a lower surface and lubricant temperature [7]. Besides that, the DLC microstructure is affected by the tribological contact conditions, which can be analyzed by means of Raman spectroscopy. Thereby, the transformation of sp^2 chain bindings into sp^2 ring bindings, reduction of density and rearrangement of sp^2 bindings and the effusion of hydrogen, only valid for hydrogen-containing DLC, can be described as shown by Kalish et al. [19]. These three steps can be summarized by the term relaxation. The Raman spectrum of amorphous carbon is characterized by the D and G peak, which arise from different vibrational states of the molecules generated by visible light (VIS) laser or ultraviolet light (UV) excitation as described by Robertson and Ferrari [20]. Changes in accordance with the relaxation can be quantified by the intensity ratios of the D and G peak, $I(D)/I(G)$, under VIS and UV excitation. The full width half maximum FWHM(G) allows the analysis of changes of bond angle and bond length distortions, so called structural disorder, in accordance with the findings of Casiraghi et al. [21]. Therein, the quotient dispersion $Disp(G)$ of the difference of the G peak positions under VIS and UV excitation divided through the difference of the excitation wavelengths is also described. It enables an analysis of the topological disorder which combines the information of size and shape distribution of sp^2 clusters of chains. Additional information regarding the Raman spectroscopy of DLC in this study are provided in [22].

Scientific studies on coated thermoplastics are currently limited mainly to applications exposed to moderate tribological stresses and standard materials such as PE. However, for the highly stressed EHL contact, occurring in machine elements as for example polymer gears, there is still comparatively limited insight into the influence of DLC coatings, especially for the relevant high-performance polymers like PA66 and PEEK. Therefore, this study investigates the

tribological behavior of DLC coated PA66 and PEEK. A related paper of the authors [22] focuses on the development and analyses of hydrogenated DLC coatings (a-C:H) for the application on thermoplastic polymers and evaluates their friction and wear behavior under dry and lubricated sliding conditions on a pin-on-plate tribometer. The development and analyses of the a-C:H coatings are explained in detail. This paper is concerned with the friction and temperature behavior of coated thermoplastic polymers under lubricated rolling-sliding conditions in a twin-disk tribometer. The a-C:H coated specimens were analyzed after tribological testing to identify possible changes in the coating structure and further correlated with findings based on frictional and wear behavior.

2 Methods

To analyze the influence of a-C-H coatings for PEEK and PA66 on the tribological behavior of lubricated rolling-sliding contacts, friction and temperature measurements are carried out at a twin-disk tribometer. Furthermore, the long-term performance in terms of wear and friction behavior of coatings is investigated and chemically analyzed following the experiments.

2.1 Twin-Disk Tribometer

The tribological investigations were carried out on a twin-disk tribometer, Fig. 1 (left). This is an analogy test rig for rolling-sliding contacts as found in machine elements like gears and roller bearings. The following description is based on Reitschuster et al. [8]. Two independently driven cylindrical disks (\varnothing 80 mm) are loaded by the adjustable normal force F_N that a pneumatic air cylinder applies to the end of a pivot arm, where the lower disk is mounted. The upper disk

is firmly fixed in a skid, which is connected to the frame via thin steel sheets. Any horizontal displacement of the skid due to frictional forces from the rolling-sliding contact is resisted and recorded via a load cell. The coefficient of friction μ relates the horizontally acting force to the contact normal force ($\mu = F_R/F_N$). To prevent starved lubrication, a steady lubricant volume of $\dot{Q} = 1.5$ l/min is injected centrally into the disk contact via an injection nozzle. Using an oil pump, the lubricant circulates in a closed circuit, containing an additional filter system and a heater to adjust the oil temperature. The control system also records the oil injection temperature ϑ_{Oil} , surface velocities v_1 and v_2 of the lower and upper disk, as well as the bulk temperature ϑ_M of the upper disk determined by an Pt-100 sensor around 4 mm underneath the polymer surface. The sum velocity $v_\Sigma = v_1 + v_2$, the sliding velocity $v_g = v_1 - v_2$ ($v_1 \geq v_2$) and the slip ratio $s = v_g/v_1$ characterize the kinematics of the disk contact. The test configuration consisting of a case-hardened uncoated lower steel disk (16MnCr5), and a coated polymer upper disk is shown in Fig. 1 (right).

Note that, the measuring principle detects only horizontally acting friction forces. Non-horizontal friction forces, which are likely to occur in highly-loaded polymer contact due to the high compliance of polymers, cannot be quantified by the load cells for F_R or F_N . Further losses, caused for example by internal damping inside the polymer, are seen in the bulk temperature. Therefore the measured coefficient of friction is referred to as μ^* in the following in analogy to the results shown in [8].

2.2 Specimens and Materials

Steel disks made of case-hardened steel 16MnCr5 were axially ground to an averaged mean arithmetic roughness of $R_a \approx 0.24 \mu\text{m}$ (roughness measurement in circumferential direction). Polymer disks were injection-molded around a

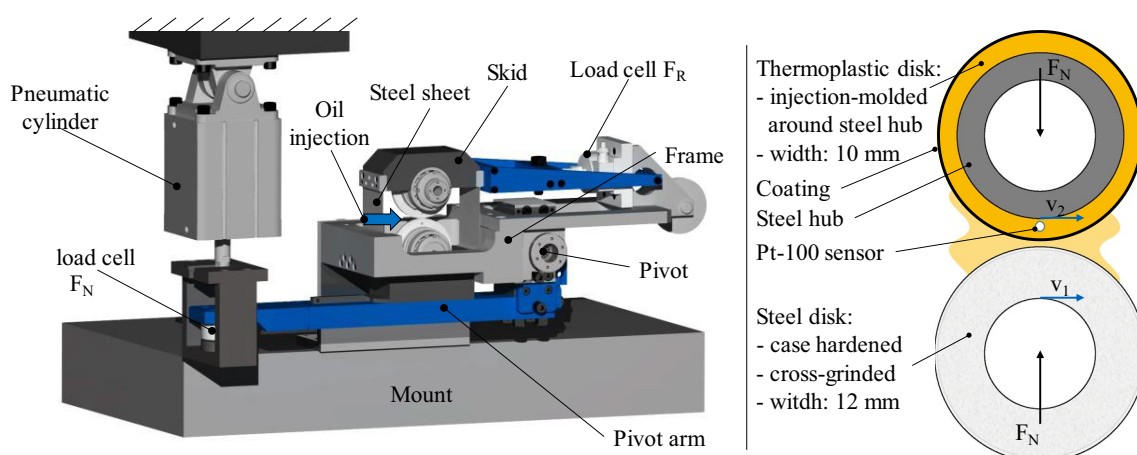


Fig. 1 Layout of the FZG twin-disk tribometer (left) and specimen design (right) in accordance with [8]

steel hub for connection to shaft in the twin-disk tribometer (see Fig. 1 right). Two thermoplastic polymers were considered: polyamide 66 (PTS–Creamid-A4H9) and polyether ether ketone (Evonik PEEK-VESTAKEEP® 4000 G). Basic material parameters for each polymer are given in Table 1 for dry conditions and at ambient temperature. Note that material properties of thermoplastics can strongly depend on the temperature and ambient conditions.

In accordance with [22] a newly developed amorphous hydrogenated carbon coating (a:C–H-1) was applied on PEEK and a:C–H-2 on PA66 by low-temperature physical vapor deposition (PVD) process. Prior to the coating process, PEEK and PA66 specimens were pretreated to improve the adhesion properties between the coating and the substrate. For this purpose, the specimens were first ground and then polished to an average surface roughness of less than $R_a < 0.1 \mu\text{m}$. The coating process itself was carried out in an industrial scale coating unit CC800/9 Custom, CemeCon AG, Würselen, Germany, with two high power pulsed magnetron sputtering (HPPMS) cathodes. The C targets used for the deposition of the a:C:H coating have a purity of C = 99.9%. As process as well as reactive gas argon (Ar), helium (He) and ethyne (C₂H₂) were used. The coatings show a columnar structure with the transition into an amorphous character of both coatings. Furthermore, measurements by means of scratchtest showed a high compound adhesion between coating and polymer. A more detailed

description of the coating process its characterization is described in [22].

An impression of the polymer surface before and after the coating is applied is given in Fig. 2. Measurements of the layer thickness t_c result in $t_c \approx 1.0$ – $2.0 \mu\text{m}$ for both coatings. The detailed characterization of the compound and the coating process are described in [22].

The measured mean arithmetic roughness R_a for both polymer materials at the process steps injection-molding, polishing, and coating is shown in Fig. 3. The measurements on the polymer surface were determined using a tactile profile method, carried out across the disk width direction with a measuring length of $L_r = 4.80 \text{ mm}$ and a cut-off wavelength of $\lambda_c = 0.80 \text{ mm}$ according to DIN EN ISO 4288 [23]. Compared to the polished state, the coating process shows an increase in the surface roughness due to the coating deposition for both materials.

Table 1 Material parameters at dry state at ambient temperature for PA66 and PEEK [35, 36]

	PA66 (Creamid-A4H9)	PEEK (VESTA-KEEP® 4000 G)
Young's modulus E in N/mm^2	3,100	3,600
Poisson number ν	0.33	0.37
Thermal conductivity λ in $\text{W}/(\text{mK})$	0.21	0.29
Glass transition temperature ϑ_G in $^\circ\text{C}$	66	143

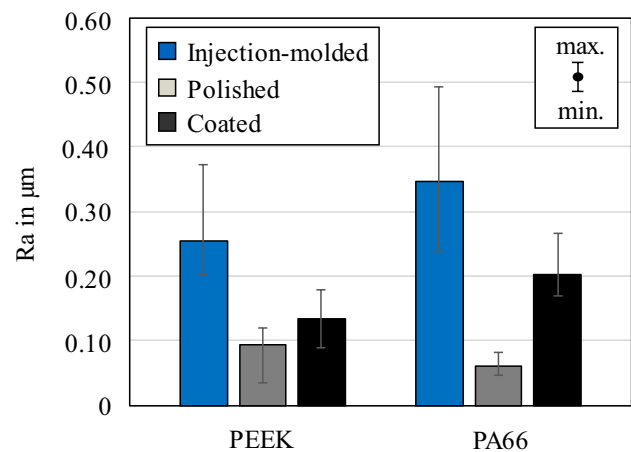


Fig. 3 Arithmetic mean roughness R_a after each process step for PEEK and PA66 disks

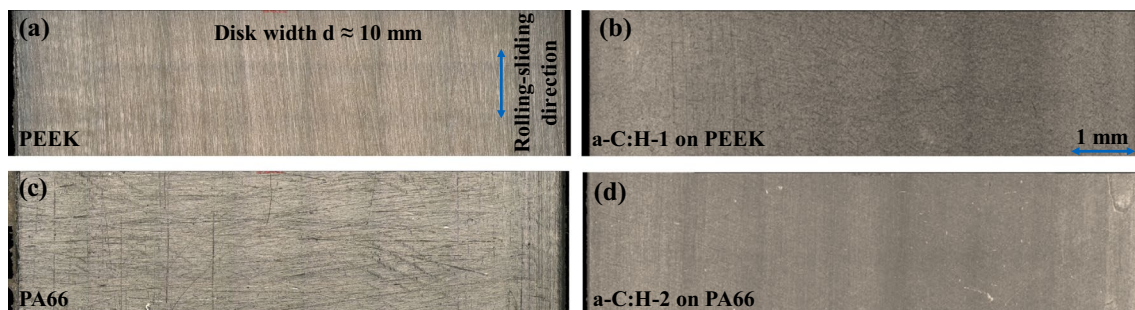


Fig. 2 Surface impression of the thermoplastic surfaces for uncoated PEEK (a); a-C:H-1 on PEEK (b); uncoated PA66 (c) and a-C:H-2 on PA66 (d)

Table 2 Properties of the mineral oil (FVA3) and water-containing polyglycol (WAT)

	FVA3	WAT
Kinematic viscosity ν (40°C) in mm ² /s	95	90
Kinematic viscosity ν (60°C) in mm ² /s	40	40
Kinematic viscosity ν (100°C) in mm ² /s	11	15
Density ρ in g/cm ³	0.90 (15°C)	1.09 (20°C)

2.3 Lubricants

The considered lubricants are mineral oil (FVA3 [24]) and a water-containing polyglycol (WAT) in analogy to [8], both are ISO VG 100. No further surface-active additives were added. An overview of the key properties of the lubricants is given in Table 2.

2.4 Chemical Analysis by Multi Wavelength Raman Spectroscopy

The molecule structure of the hydrogen-containing amorphous carbon coatings before and after tribological tests were analyzed by means of Raman spectroscopy. Therefore, the Raman spectroscope, Renishaw InVia Reflex, Renishaw GmbH, Pliezhausen, Germany, with a $\lambda_{VIS} = 532$ nm laser with a spot size of $d \approx 1$ μm and a diffraction grating of $g_{VIS} = 1,800$ l/mm was used. In addition, Raman spectra were taken with an ultraviolet (UV) laser $\lambda = 325$ nm with a spot size of $d \approx 6$ μm and a diffraction grating of $g_{UV} = 2,400$ l/mm. The lasers were calibrated before the measurement by using a silicon reference sample. To enable an evaluation of statistically valid data, a mapping measuring method was used. Hereby, a matrix with 1×8 measurement points with size of $1 \mu\text{m} \times 1,750 \mu\text{m}$ and a step width of $250 \mu\text{m}$ is positioned horizontally over the middle of the running surface of the a-C:H coated disk for the analysis by UV laser. Furthermore, a matrix with 2×3 measurement points with a size of $100 \times 160 \mu\text{m}$ and a step width of $80 \mu\text{m}$ is positioned horizontally over the middle of the running surface of the a-C:H coated disk using the $\lambda_{VIS} = 532$ nm laser. The measurement parameters are shown in Table 3.

All spectra are taken using the software Wire® 5.4, Renishaw plc, Wotton-under-Edge, United Kingdom. Thereby, the spectra are evaluated section by section of the Raman shift by a combined Gaussian and Lorentzian fitting. Based on the measured spectra the parameters $I(D)/I(G)_{VIS}$ ratio, $I(D)/I(G)_{UV}$ ratio, $FWHM_{UV}(G)$ and $Disp(G)$ are determined. In case of the characteristic value $FWHM(G)_{UV}$, the UV excitation enables to exclude the photoluminescence of the spectra as shown by Casiraghi et al. [21]. Furthermore, the dispersion of the G peak $Disp(G)$ can be calculated by determining the difference of the position at visible $\tilde{\nu}_G$ and

Table 3 Raman measurement parameters for chemical analysis of a-C:H coatings before and after tribological testing

	Vis	UV
Wavelength λ in nm	532	325
Laser power P_L in mW	2.6	3
Accumulations N	1	3
Exposure time t_E in s	10	10

UV $\tilde{\nu}_{G,UV}$ excitation divided through the difference of the excitation wavelengths.

$$Disp(G) = \frac{\tilde{\nu}_{G,UV} - \tilde{\nu}_G}{\lambda_{UV} - \lambda} \left[\frac{cm^{-1}}{nm} \right] \quad (1)$$

Based on the coating analysis in [22] the interpretations of the a-C:H coatings are orientated on the findings of Casiraghi et al. [21]. Correspondingly, the coatings were classified as graphite-like a-C:H (GLCH) with a hydrogen content $\Psi > 20\%$ and sp^2 -clustered ring bindings.

2.5 Operating Conditions and Experimental Procedure

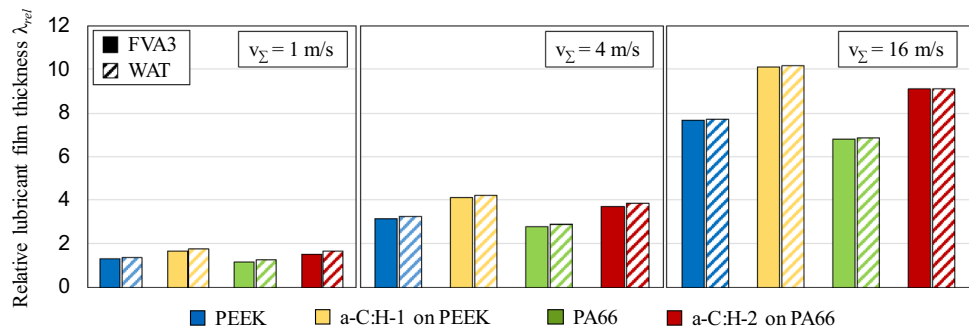
The operating conditions are chosen in analogy with previous investigations on uncoated polymers in [8] to ensure comparability are shown in Table 4. Using Hertzian theory, the Hertzian pressure for a load of $F_N = 1000$ N corresponds to $p_H = 81$ MPa for PEEK and $p_H = 74$ MPa for PA66. Numerical studies indicate that the influence of a coating on the contact stiffness and thus on the contact pressure is negligible for practical PVD coating thicknesses [7, 18].

Friction is investigated by stepwise increase of the slip ratio at a constant sum velocity and normal load (friction curve). Each time a quasi-stationary state is reached for a slip ratio, defined by a bulk temperature change of less than 0.5 K per minute ($\Delta\vartheta_M \leq 0.5$ K/min), the slip ratio is increased as shown in Table 4. The coefficients of friction μ^* and the bulk temperatures ϑ_M are averaged values over one minute in quasi-stationary state.

The lubrication regime for different operating conditions is approximated by the relative film thickness $\lambda_{rel} = 2 \cdot h_m / (Ra_1 + Ra_2)$. Therein, the minimum film thickness h_m is calculated according to Myers et al. [25]. For the associated Ra values, the disk surface roughnesses in the initial state are used (see Fig. 3). The determined relative film thicknesses λ_{rel} are shown in Fig. 4. A low sum velocity of $v_\Sigma = 1$ m/s results in a relative lubricant film thickness $\lambda_{rel} < 2$ for all materials, which can be associated with the mixed lubrication [26]. Higher sum velocity leads to an increase in the relative lubricant film thickness λ_{rel} . Fluid film lubrication is assumed for a relative lubricant film thickness $\lambda_{rel} > 2$.

Table 4 Operating conditions for investigations on the FZG twin-disk tribometer

	Friction curves	Long-term tests
Normal force F_N in N	1,000	
Sum velocity v_Σ in m/s	4/1/16	1
Slip ratio s in %	0/5/10/20/30/40/50/60/70	50
Lubricant	FVA3; WAT ($\vartheta_{Oil} = 60^\circ\text{C}$)	FVA3 ($\vartheta_{Oil} = 60^\circ\text{C}$)
Material	PEEK; PA66	
Surface finish	Uncoated (injection-molded); a-C:H-1 coating (on PEEK); a-C:H-2 coating (on PA66)	
Setup of disks	Polymer-steel contact	

Fig. 4 Relative lubricant film thickness λ_{rel} for uncoated and coated PEEK/PA66 with FVA3 and WAT

In the preparation of each friction test, the disks were thermally conditioned through oil injection at $v_\Sigma = 1$ m/s and no-load conditions to achieve quasi-stationary bulk temperatures $\vartheta_{M,0}$ ($\vartheta_{Oil} = 60^\circ\text{C}$) $\approx 34\text{--}35^\circ\text{C}$. In total, a test cycle consists of the three different sum velocities ($v_\Sigma = 1, 4, 16$ m/s), whereby each sum velocity was in total repeated three times. The first sum velocity is $v_\Sigma = 4$ m/s, followed by $v_\Sigma = 1$ m/s and $v_\Sigma = 16$ m/s. The first of three runs at $v_\Sigma = 4$ m/s were not used for the evaluation of the results, as it is considered as a conditioning run. A further running-in process was not performed. After each of the described test cycle, new pairings of test specimens were used.

For the investigation of the long-term performance under critical lubrication conditions, tests were conducted at mixed lubrication at $v_\Sigma = 1$ m/s and a slip ratio $s = 50\%$ over a period of $t = 8$ h. Hereby the focus was on the development of the coefficient of friction over time as well as changes of the surface condition and possible wear marks. The surface condition were examined each time before and after the long-term tests by means of high-resolution images and roughness measurements.

3 Results and Discussion

The following results shows the tribological performance of coated thermoplastic polymers as measured at the twin-disk tribometer. For the sake of comparability, results for uncoated polymers under tribological conditions from [8] are included.

3.1 Friction and Temperature Behavior in Friction Curves

This section shows results of the friction curve measurements by illustrating the coefficient of friction μ^* and the bulk temperature ϑ_M for variation of the slip ratio s . Hereby, the coefficient of friction μ^* is mainly related to the interfacial friction from the disk contact (see Sect. 2.1).

3.1.1 Influence of Operating Conditions and Material

First, the influence of the a-C:H coatings on the friction and temperature behavior at different sum velocities is

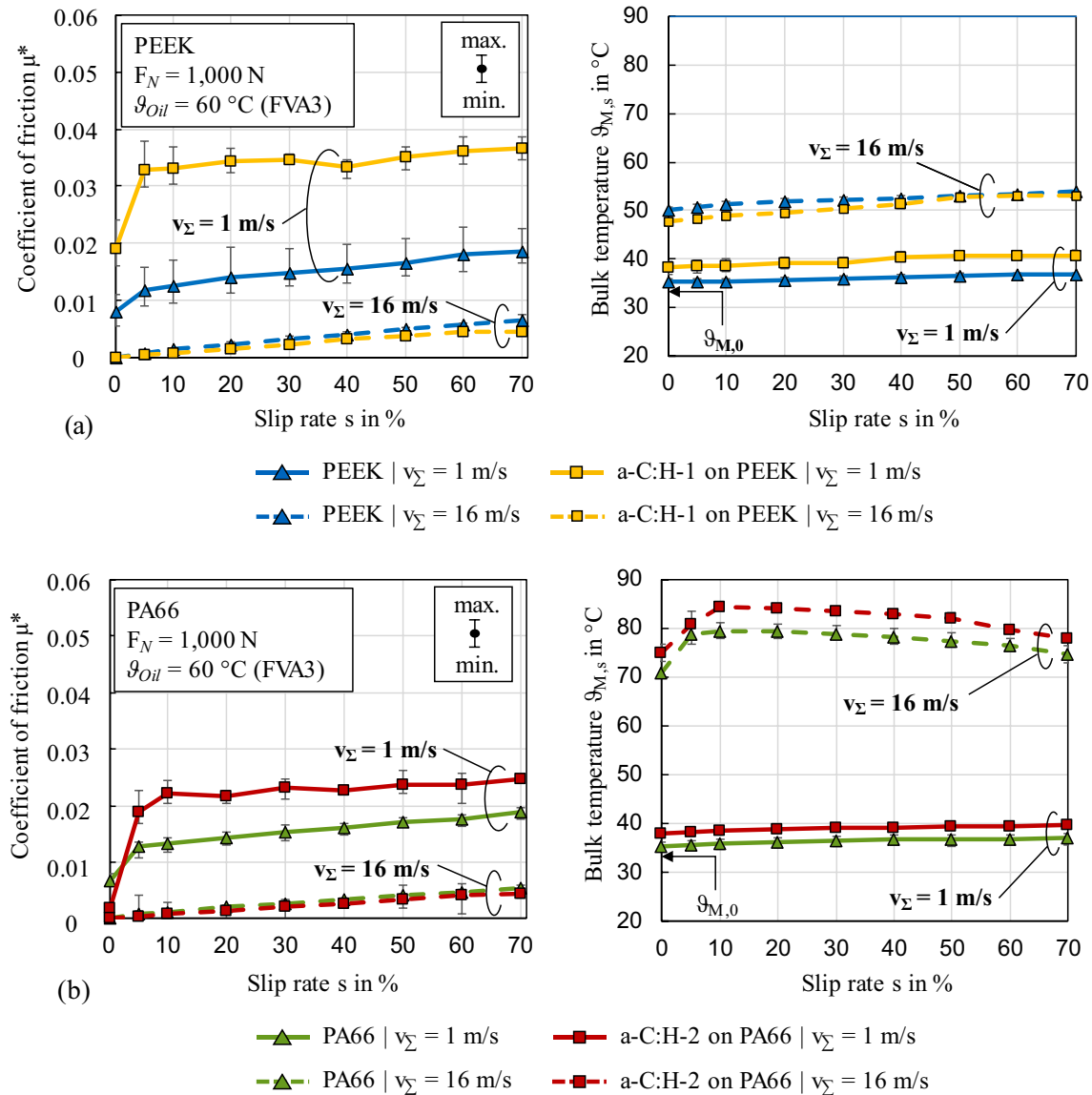


Fig. 5 Friction and temperature behavior of uncoated [8]/coated PEEK (a) and PA66 (b) for different sum velocities v_{Σ} with mineral oil FVA3

considered for mineral oil FVA3 in Fig. 5. Under conditions with fluid film lubrication ($v_{\Sigma} = 16$ m/s, $\lambda_{rel} > 2$, see Fig. 4), friction is characterized by very low coefficients of friction μ^* for both materials. Coated and uncoated variants of PEEK and PA66 show both a linearly rising friction curve with increasing slip rates. This indicates that the effective viscosity in the contact region remains low which agrees with [7, 18] where no relevant influence of the coating thickness on the contact stiffness was detected. However, in mixed lubrication regime ($v_{\Sigma} = 1$ m/s, $\lambda_{rel} < 2$, see Fig. 4), differences can be seen between the coated and the uncoated variants regarding the frictional behavior. The uncoated PEEK as well as the uncoated PA66 show overall lower coefficients of friction and comparable friction curves with a continuous gradient for increasing slip

ratios. Although the surface roughness of the coated variants is lower (see Fig. 3), higher interfacial friction for coated PA66 (a-C:H-2 on PA66) and especially for coated PEEK (a-C:H-1 on PEEK) is observed. For both coated variants, the friction curve is characterized by a rapid rise at the transition from pure rolling to rolling-sliding conditions. Afterwards, both friction curves become almost steady, which indicates nearly constant shear stress and interfacial friction despite increasing sliding velocity. Similar results were found in a pin-on-plate tribometer configuration [22]. To exclude delamination of the coating and inspect the coating for possible changes as a result of the high loading stress, the condition of the surfaces were examined in each case using Raman spectroscopy and SEM microscopy (see Sect. 4.2).

The corresponding bulk temperatures ϑ_M shows for uncoated and coated variants an increase of the bulk temperature depending mainly on the loading frequency and hardly on the slip ratio. PA66 has a significantly higher increase in bulk temperature in contrast to PEEK. Despite different coefficients of friction between uncoated and coated polymer, the impact of the coating on the bulk temperature is small. Indications of an thermal insulation effect like in DLC-coated steel contacts under elastohydrodynamic lubrication as shown in [27] cannot be observed. This is related with similar thermal effusivities of the a-C:H coatings and the considered polymers. However, as Ziegler et al. [7] have shown, a marginal reduction in the polymer/steel contact temperature directly at or just below the surface is possible.

A direct correlation between interfacial friction and bulk temperature cannot be determined. Instead, the internal solid losses appear to be the dominant influencing factor on the bulk temperature for both coated and uncoated polymers. This is in agreement with the results in [7], which have shown that the mechanical characteristics, like the overall contact stiffness and the associated material elongation of the polymers are hardly affected by the coating. Therefore, in accordance with Sect. 1, PA66 reaches significantly higher bulk temperatures than PEEK, due to its more pronounced damping behavior compared to PEEK. Marginal differences in the measured bulk temperatures between uncoated and coated variants are attributed mainly to the ambient influences during the test procedure.

3.1.2 Influence of the Lubricant

In addition to the mineral oil FVA3, a water-containing fluid (WAT) is considered at an oil temperature of $\vartheta_{Oil} = 60^\circ\text{C}$. The coefficients of friction μ^* for uncoated and a-C:H-1 on PEEK in the mixed lubrication regime ($v_\Sigma = 1$ m/s) is shown in Fig. 6 for both lubricants. The results with the mineral oil FVA3 follow the linear increase of the coefficient of friction with slip ratio and a strong increase as soon as a sliding velocity is applied.

In direct comparison, the water-containing fluid WAT shows significantly lower interfacial friction under the same operating conditions. According to Chen et al. [28–30], a possible reason for this is the friction-reducing formation of a microscopic layer of FeOOH on the steel counter-part in ambient conditions, accumulating a hydrogen-bonded film of glycol and free water molecules. Besides, also the almost 20% higher density of WAT compared to FVA3 can enhance the formation of the lubricant film by increasing the film thickness up to 10% according to Myers et al. [25]. Due to low pressure conditions, the influence of the pressure viscosity coefficient on the lubricant film thickness is comparably small. As a result, the relative lubricant film thickness for a-C:H-1 on PEEK/steel increases from $\lambda_{rel,FVA3} = 1.69$

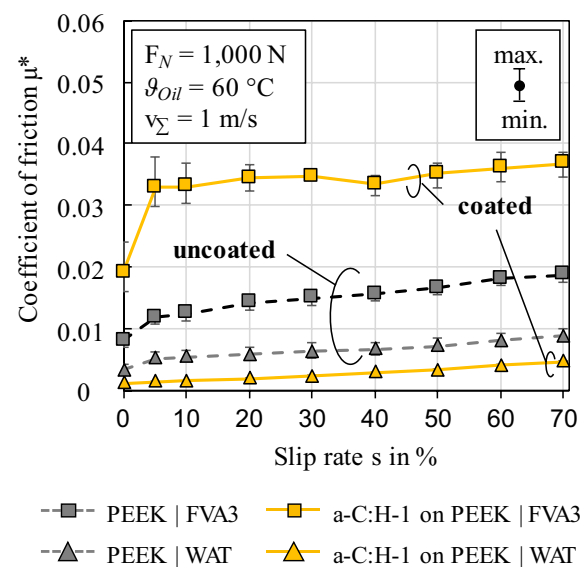


Fig. 6 Friction behavior of uncoated [8]/coated PEEK in comparison of different lubricants

to $\lambda_{rel,WAT} = 1.77$ ($v_\Sigma = 1$ m/s), which indicates a decreasing interfacial friction. Presumably, due to the lower surface roughness compared to the uncoated PEEK, a-C:H-1 on PEEK additionally leads to reduced interfacial friction in mixed lubrication. In combination with the water-containing lubricant, this results in very low coefficients of friction in the range of superlubricity despite the present mixed lubrication regime.

3.1.3 Influence of Conditioning Run

In contrast to one conditioning run at $v_\Sigma = 4$ m/s and subsequent measurements at $v_\Sigma = 4$ m/s, $v_\Sigma = 1$ m/s and $v_\Sigma = 16$ m/s (see Sect. 3.1.1), the conditioning procedure was changed to one conditioning run at $v_\Sigma = 1$ m/s followed by measurements at $v_\Sigma = 1$ m/s, $v_\Sigma = 4$ m/s and $v_\Sigma = 16$ m/s. All other operating conditions remained the same (see Table 4). For “slow” conditioning at $v_\Sigma = 1$ m/s, mixed lubrication is present and the sliding velocities are low. “Fast” conditioning at $v_\Sigma = 4$ m/s shows fluid film lubrication and high sliding velocity. Hence, “fast” conditioning comes along with zero specific boundary friction power [31]. The terms “fast” and “slow” are kept in the following. Figure 7 presents the coefficients of friction for both conditioning procedures.

In mixed lubrication at $v_\Sigma = 1$ m/s, the “slow” conditioning shows lower coefficients of friction than the “fast” conditioning for both coating variants. The observed effect is more pronounced for a-C:H-1 on PEEK (see Fig. 7 (a)). However, in the area of fluid film lubrication ($\lambda_{rel} > 2$) at $v_\Sigma = 4$, no effect of the different conditioning processes can be seen. While the conditioning of the surfaces does

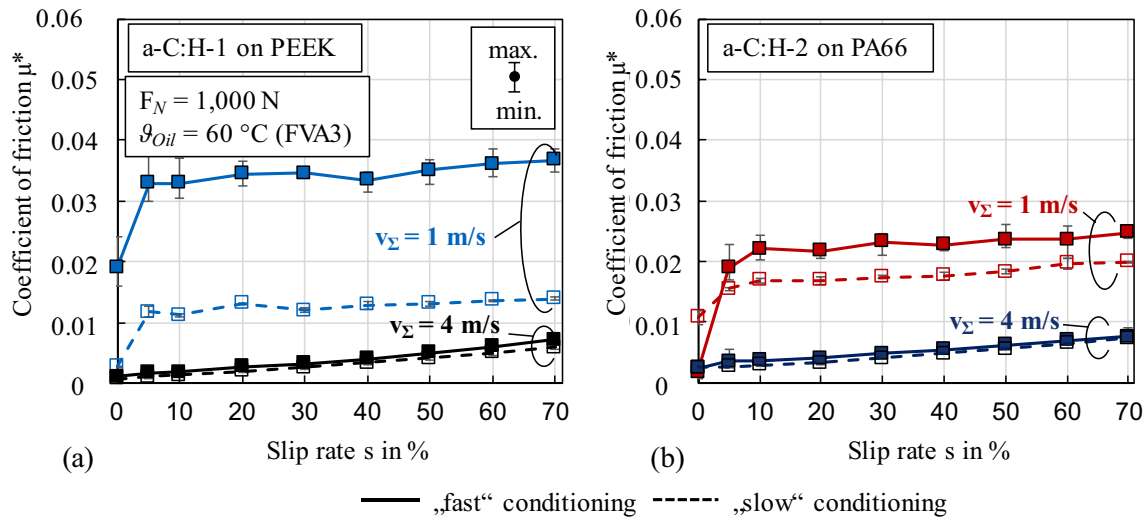


Fig. 7 Friction behavior of coated PEEK (a) and coated PA66 (b) for different conditioning procedures ($\theta_{Oil}=60^{\circ}\text{C}$; $F_N=1,000\text{ N}$; FVA3)

not seem to affect friction in fluid film lubrication, the coefficients of frictions differ in mixed lubrication. It appears that a “fast” conditioning causes an alternation of the surfaces that prohibits low friction in the subsequent measurement at $v_{\Sigma}=1\text{ m/s}$. The cause of the alternation could be found in the higher sliding velocity and the associated frictional power. The coating structure and chemistry was analyzed in detail for further insight (see Sect. 4.2). In this case, it appears that the “slow” conditioning improves the tribological performance of the coating.

3.2 Long-term Tests under Critical Lubrication Conditions

It has been shown that surface wear increasingly becomes a relevant damage type under severe lubrication condition for polymer/steel contacts [3]. The long-term performance of the two developed a-C:H coatings was tested with regard to friction reduction and wear protection of the polymers PEEK and PA66 under severe mixed lubrication. Therefore, tests were carried out for 8 h under constant normal force of $F_N=1000\text{ N}$ (no previous running-in procedure), an oil injection temperature of $\theta_{Oil}=60^{\circ}\text{C}$, a sum velocity of

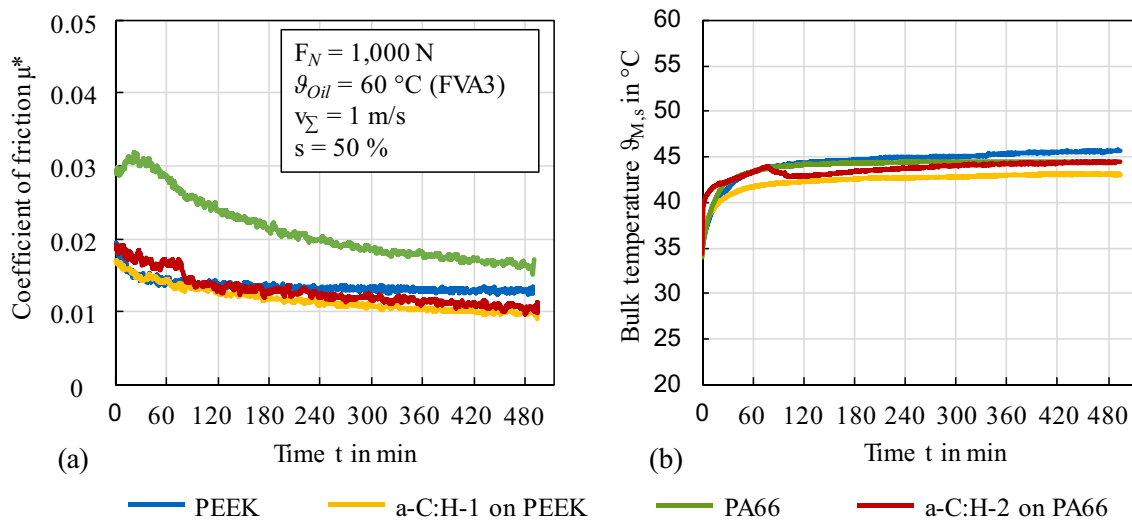


Fig. 8 Friction (a) and temperature behavior (b) over time in comparison of uncoated and coated PEEK/PA66

$v_{\Sigma} = 1$ m/s and a high slip ratio of $s = 50\%$. The corresponding measured coefficients of friction and bulk temperatures for the coated and uncoated PEEK and PA66 are shown in Fig. 8.

Considering the entire test period, all variants show a decrease in the coefficient of friction μ^* . The high coefficient of friction of uncoated PA66 can be related to the comparatively high initial surface roughness (see Fig. 3; condition: injected-molded) and reduces over the entire runtime, indicating a non-stationary surface state. The coefficient of friction of uncoated PEEK is characterized by a stable development after a short conditioning phase. The comparison of a-C:H-1 on PEEK and a-C:H-2 on PA66 shows a similar development of the coefficients of friction. They continuously decrease to a level below the ones of uncoated PEEK and PA66. Finally, the coefficients of friction for both coated variants are at an almost identical value of approximately $\mu^* \approx 0.01$. Please note, a direct comparison with the results shown in chapter 3.1 is basically not possible, since different test procedures are used. In particular, the disk conditioning, which has an influence on the friction behavior, is different in the two procedures (see Table 4). Besides the coefficient of friction, the corresponding bulk temperature for all variants

is shown Fig. 8 (b). Despite the different coefficients of friction, all variants show a comparable temperature behavior. After a temperature increase at the beginning, the bulk temperature reaches an almost stationary value in the following test period. The differences between the variants are small, and can be attributed to external ambient influences. As already described in Sect. 3.1.1, indications that the coatings effect the bulk temperature cannot be determined here either. For the evaluation of the surface condition, high-resolution images of the disk surface before and after the test were recorded, complemented by information on the surface roughness for each state. Topography images before and after the test runs for coated and uncoated PEEK and PA66 are shown in Fig. 9.

In the long-term tests, the surfaces of uncoated PEEK and PA66 show clear signs of wear in the form of markers and grooves along the circumferential disk direction. These are more pronounced for PA66, which agrees with roughness measurements shown in Fig. 10. However, despite the significant increase in surface roughness for both uncoated variants, no increase in the coefficient of friction can be detected during the test run. In contrast to the uncoated disks, both a-C:H coated disks provide an effective wear protection under these conditions, as

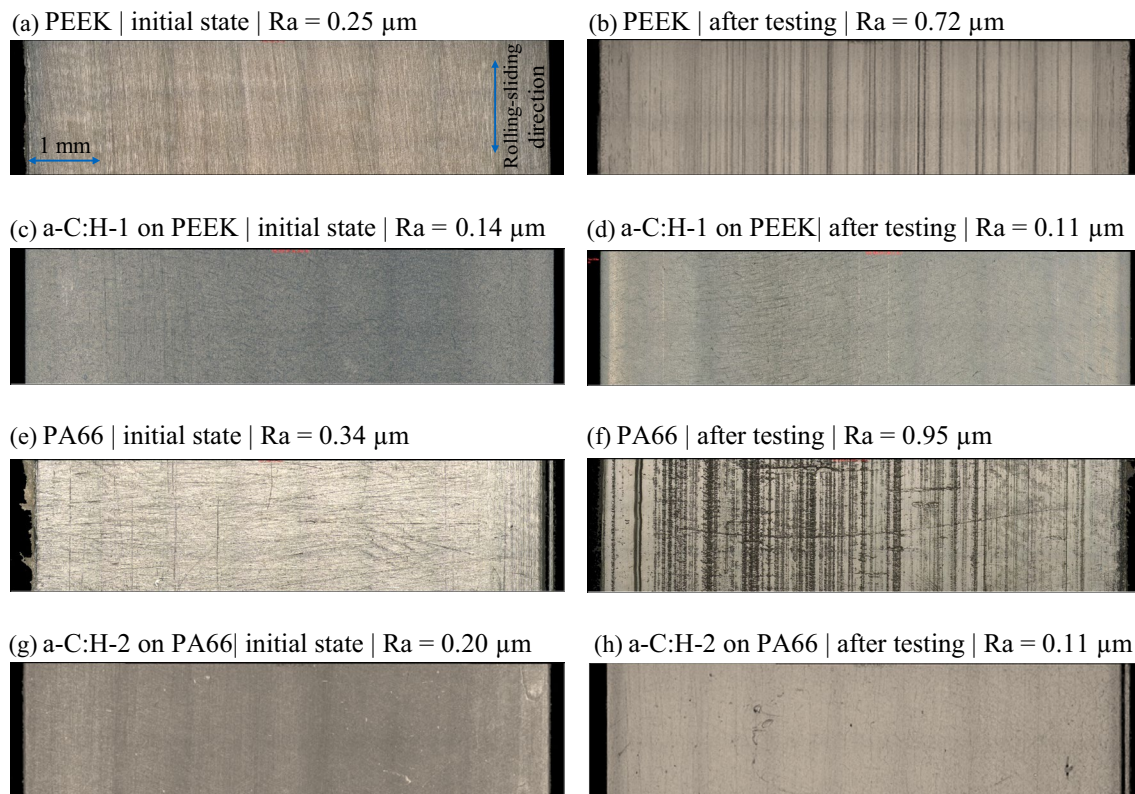


Fig. 9 Topography of uncoated and coated PEEK (a–d) and PA66 (e–f) before and after the long-term tests

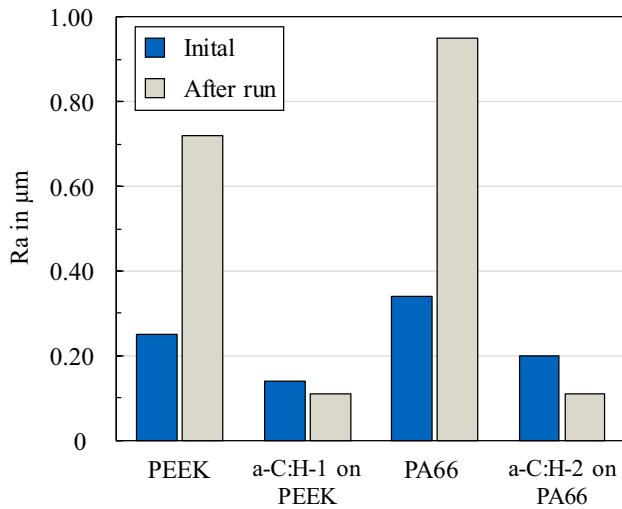
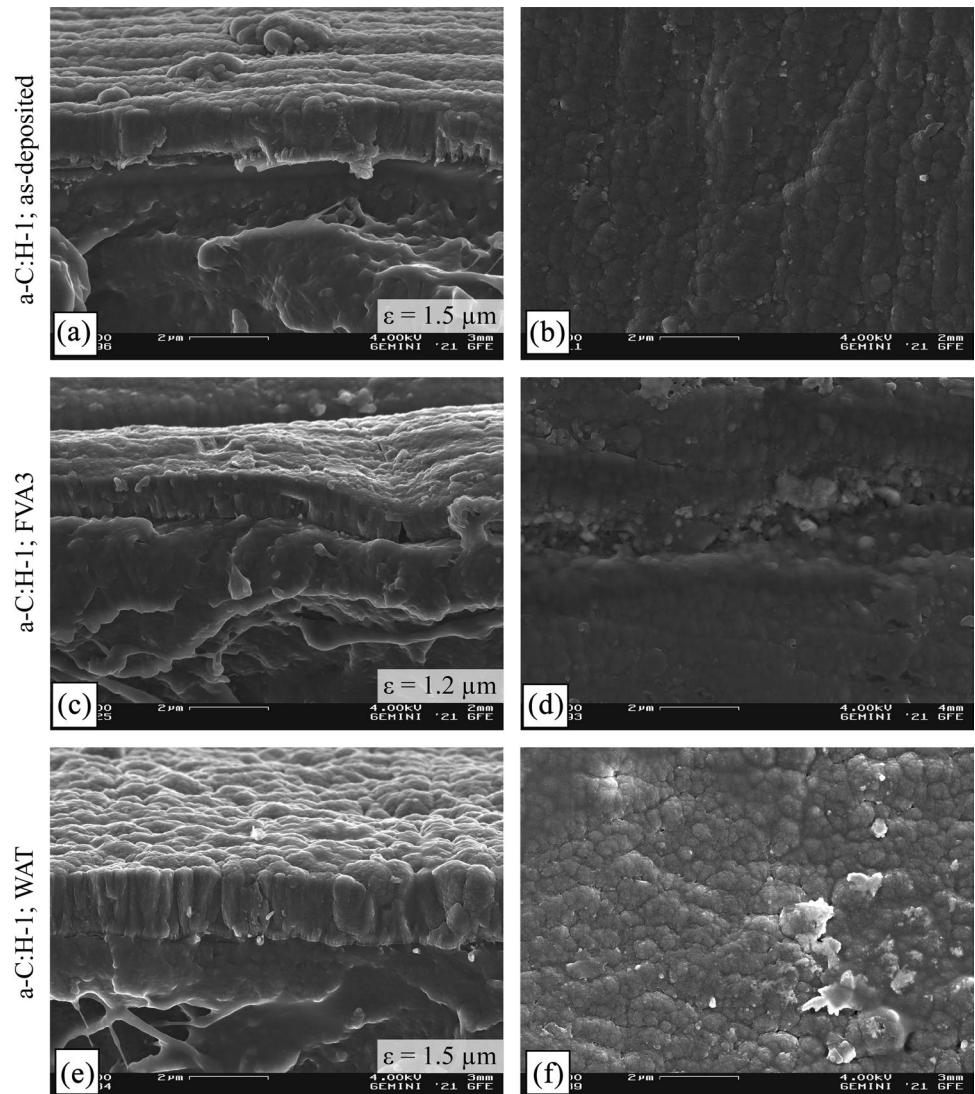


Fig. 10 Comparison of surface roughness before and after the long-term tests

no indication of wear marks on the coated surfaces can be detected. The corresponding roughness measurements confirm this impression with decreasing surface roughness values Ra and Rz. This is consistent with the coefficient of friction curves shown in Fig. 8.

Any signs of damages or delamination of the coating, which are possible due to the applied high stress level could not be detected, either. This is seen as an indication for a high compound adhesion between coating and polymer and an effective protection of the soft thermoplastic polymer surfaces by the DLC coatings. Previous experimental investigations on a ball-on-plate tribometer [32] confirm the wear-reducing effects of a-C:H-1 on PEEK for the material PEEK.

Fig. 11 Cross-sectional micrographs (a, c, e) and topography (b, d, f) of a-C:H-1 coated PEEK disks at centre of disks as-deposited and after lubricant variation and fast conditioning



4 Structural and Chemical Analysis of Coated and Uncoated Polymer Disks after Tribological Testing

4.1 Characterization of Disk Topography after Lubricant Variation

The cross-section and topography of a-C:H-1 on PEEK in the states coating as-deposited and after tribological testing under FVA3 and WAT lubrication and fast conditioning are shown in Fig. 11 (see Sect. 3.1.2). By comparing both tribological contacts and the as-deposited status, no changes of the columnar and amorphous coating structure could be observed.

Nevertheless, the a-C:H-1 on PEEK coating on thickness ϵ after friction curve measurements with FVA3 is significantly reduced from $\epsilon = 1.5$ to $\epsilon = 1.2$ μm (Fig. 11 (a); (c)) compared to the measurements with WAT (Fig. 11 (a), (e)). However, the columnar structures of all tested and untested a-C:H-1 on PEEK coatings remain unchanged. An effect of a slow conditioning process (see Sect. 3.1.3) on the coating structure of a-C:H-1 on PEEK cannot be observed, Fig. 12. The dense and amorphous structure does not change after slow conditioning with regard to the cross section. In contrast, the columnar appears to be coarser compared to the structure after fast conditioning. Nevertheless, the coating thickness remains unchanged with $\epsilon = 1.5$ μm after slow conditioning, whereas during fast conditioning the coatings thickness was reduced from 1.5 μm to 1.2 μm . The topography of the a-C:H-1 on PEEK coating after slow conditioning (see Fig. 12) shows a smooth top layer like a-C:H-1 on PEEK after fast conditioning (see Fig. 11 (c)).

Figure 13 presents the a-C:H-2 on PA66 coating after fast and slow conditioning. Here, the coating thickness of a-C:H-2 on PA66 after slow conditioning is reduced from $\epsilon = 1.8$ μm (see Fig. 13 (a)) to $\epsilon = 1.4$ μm (see Fig. 13 (e)), but only slightly reduces to $\epsilon = 1.7$ μm after fast conditioning (see Fig. 13 (c)). By comparing the morphologies

of the a-C:H-2 on PA66 coatings initially and after fast conditioning, no modifications can be observed. On the other hand, the columnar morphology of a-C:H-2 on PA66 coating after slow conditioning appears to be coarser as already seen for a-C:H-1 on PEEK. It has to be stated, that based on the SEM cross section no clear interpretation is possible. Besides the coating topography after the conditioning, the bonding structure could also affect friction in mixed lubrication. Therefore, the next step is to consider the effect of the tribological contact conditions on the coatings structure by means of Raman spectroscopy. Here, the focus was set on the different conditioning processes fast and slow with a-C:H-1 on PEEK and a-C:H-2 on PA66 under FVA3 lubrication.

4.2 Chemical Analysis of the Coatings by means of Raman Spectroscopy

Figure 14 represents the evaluated D peak and G peak intensity ratios $I(D)/I(G)$ under UV and VIS excitation for a-C:H-1 on PEEK and a-C:H-2 on PA66 before and after the friction curve measurements. The $I(D)/I(G)_{UV}$ ratios show an increasing tendency for a-C:H-1 on PEEK and a-C:H-2 on PA66, which reach the highest values under fast conditioning. The ratio is lower for both a-C:H coatings under slow conditioning. Opposite to this, a clear trend cannot be found with regard to the $I(D)/I(G)_{VIS}$ ratios of a-C:H-1 on PEEK and a-C:H-2 on PA66. With regard to the evaluation of a-C:H coatings, the relevance of UV spectra is higher in favor of the visible spectra, which was also concluded in the studies of Casiraghi et al. [21] as well as Ferrari and Robertson [33]. One reason is the impact of photoluminescence (PL), valid for a-C:H coatings with high hydrogen content $\Psi > 40\%$, on the Raman spectra under visible excitation, which lead to a less characteristic spectrum compared to UV excitation. Moreover, the dominance of the sp^2 cross section under visible excitation, limit the analysis of sp^3 like C-H_x bonds and sp^3 C-C bonds. Therefore, the following conclusion will be based on the $I(D)/I(G)_{UV}$ ratios.

Fig. 12 Cross-sectional micrographs and topography of a-C:H-1 on PEEK disks at centre of disks after slow conditioning process

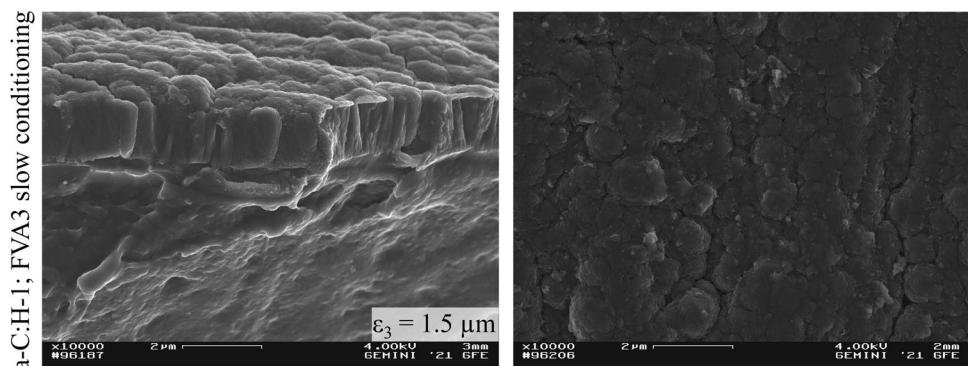


Fig. 13 Cross sectional micrographs (a, c, e) and topography (b, d, f) of a-C:H-2 on PA66 disks at centre of disks as-deposited and after conditioning process variation

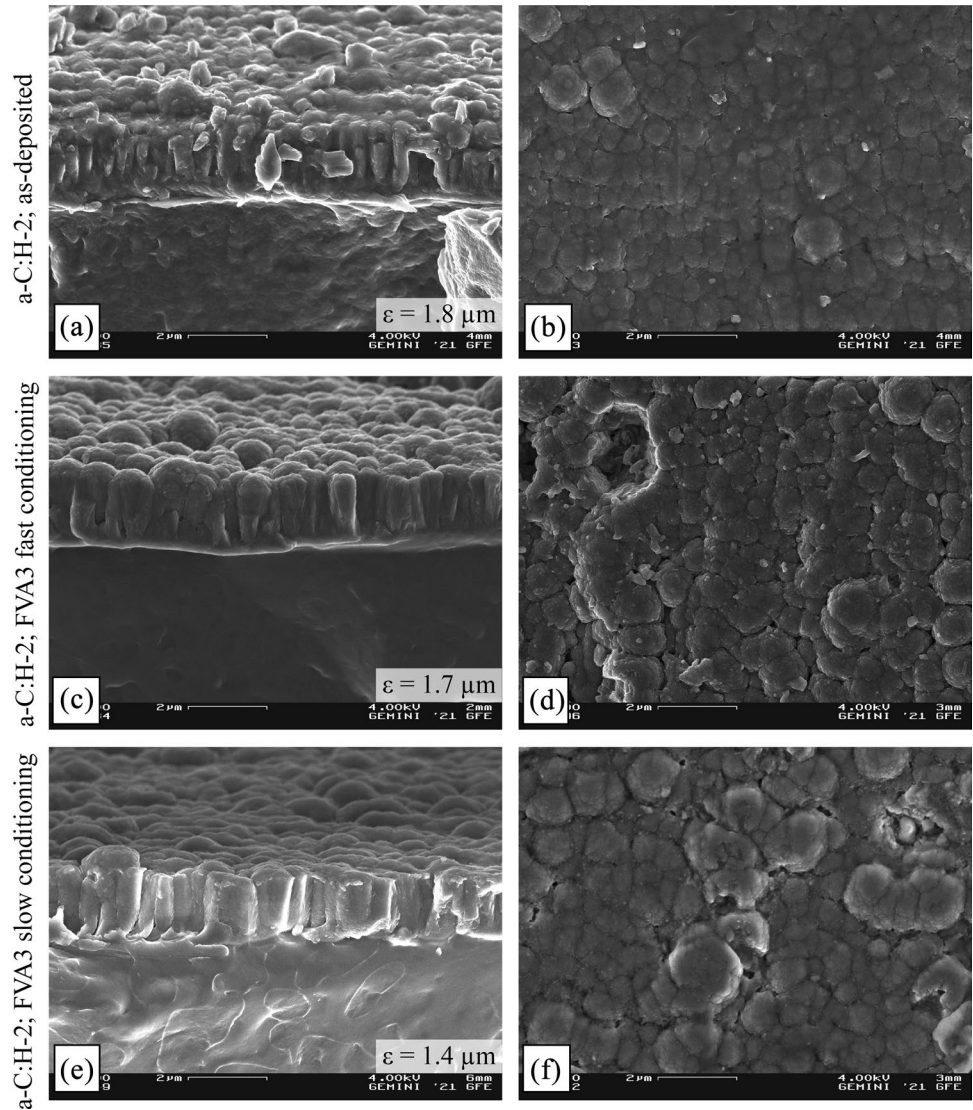


Fig. 14 $I(D)/I(G)_{UV}$ and $I(D)/I(G)_{VIS}$ ratios of a-C:H-1 on PEEK and a-C:H-2 on PA66 as-deposited and after fast and slow conditioning under FVA3 lubrication

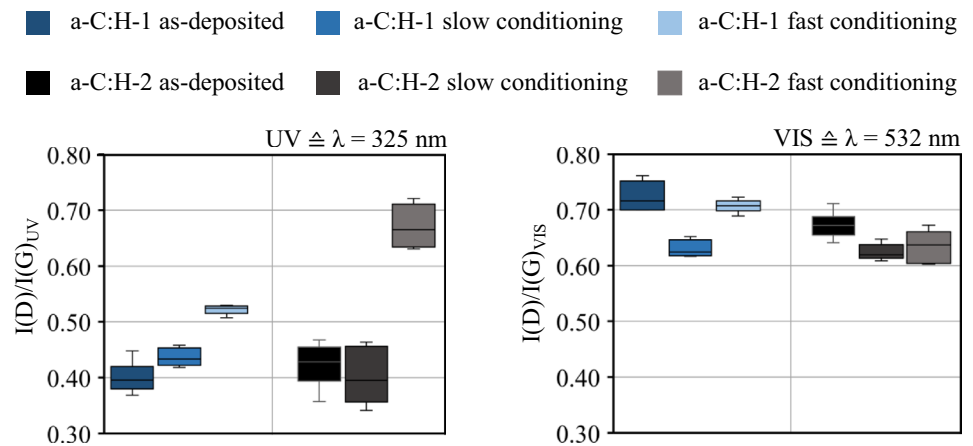
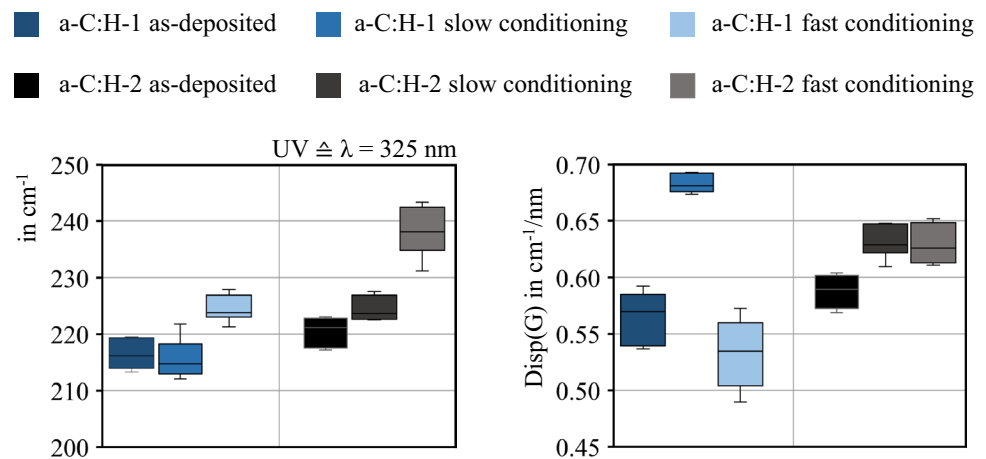


Fig. 15 FWHM(G)_{UV} and Disp(G) of a-C:H-1 on PEEK and a-C:H-2 on PA66 as-deposited and after fast and slow conditioning under FVA3 lubrication



Both a-C:H coatings are a combination of sp^2 -ring bindings from sputtered graphite and chain bindings from the use of ethyne during the coating process. The latter is proven by the appearance of the D peak for all considered spectra under UV excitation. Furthermore, the increase of the $I(D)/I(G)_{UV}$ ratios after tribological testing prove the initiation of a relaxation and in particular by fast conditioning. A first conclusion based on the increasing $I(D)/I(G)_{UV}$ ratio, is the transformation from sp^2 -chain into sp^2 -ring bindings. In order to differentiate more precisely how clustering as subprocess of relaxation is affected, FWHM(G)_{UV} and Disp(G) are determined for a-C:H-1 on PEEK and a-C:H-2 on PA66, Fig. 15. These characteristic values enable to set the focus on the process of rearrangement of the sp^2 bindings.

By taking the FWHM(G)_{UV} and Disp(G) of a-C:H-1 on PEEK under slow conditioning into account, the results reveal less changes in the structural disorder but an increase of the topological disorder. This means that the bonding lengths and angles are hardly affected, whereas the size and distribution of the sp^2 -clusters have changed in comparison to the initial state. For fast conditioning of the a-C:H-1 on PEEK coating, the structural disorder is increased and the topological disorder tends to ordering. Overall, the percentage changes of the a-C:H-1 on PEEK bonding structure under slow conditioning are greater towards the effect of fast conditioning on the bonding structure of a-C:H-1.

In case of a-C:H-2 on PA66, both types of disorder are independently affected by the conditioning as shown by an increase of the characteristic values FWHM(G)_{UV} and Disp(G). The significant difference between the influence of fast and slow conditioning is found in the magnitude of the absolute values of FWHM(G)_{UV}. Here, the influence of the fast conditioning leads to an increase in column width, which can also be observed in the SEM cross-section. The results show, that differing tribological conditions lead to a deviating rearrangement of the binding structure as well as the possible transformation from chain to ring bindings. It

can be concluded, that the process of clustering is differently affected by the tribological conditioning. A transformation of sp^2 chain into sp^2 ring bindings and a rearrangement by topological and structural disordering is proven. A statement about the percentage shares of the mechanisms of clustering in each case is not possible. The effusion of hydrogen cannot be clarified as well as the possible transformation of diamond-like sp^3 bindings into graphitic sp^2 bindings, which are also a part of the relaxation process. However, the last-mentioned is less sensitive to low energy inputs and requires higher temperatures or loads than present in contacts with thermoplastic polymers.

4.3 Correlation of Tribological Testing and Chemical Analysis

The correlation of the coefficient of friction and structural analyses through Raman spectroscopy allows a deeper interpretation of the molecular adhesion and its effect on friction. The measured roughness of coated disks before tribological testing show arithmetic roughness values of $R_a = 0.2 \mu\text{m}$ for a-C:H-2 on PA66 and $R_a = 0.14 \mu\text{m}$ for a-C:H-1 on PEEK. After tribological testing the roughness values of a-C:H-1 on PEEK and a-C:H-2 on PA66 are reduced to a value of $R_a = 0.11 \mu\text{m}$. Based on this, the solid load portion and therefore the influence of solid contacts on the coefficient of friction is expected to be higher for a-C:H-2 on PA66/steel compared to a-C:H-1 on PEEK/steel.

With regard to the measured coefficient of friction, the lowest values for FVA3 lubrication were measured for a-C:H-1 on PEEK and a-C:H-2 on PA66 under slow conditioning. It is noticeable, that for these coatings the structural disorder is not as high as it is for the coatings under fast conditioning. Moreover, both a-C:H coatings show an increase of the topological disorder under slow conditioning. It can be concluded that the structural disorder has a greater influence on the friction reduction compared to the topological

disorder. Furthermore, the impact of the conditioning procedure on the coefficients of friction are greater for a-C:H-1 on PEEK than for a-C:H-2 on PA66. A distinction between the coatings can also be made based on the $\text{Disp}(G)$, which differs significantly for a-C:H-1 on PEEK, whereas the values of a-C:H-2 on PA66 are at a similar level.

Based on the discussed results, the following mechanism is proposed. The boundary friction power and shear stress initiate topological disordering under slow conditioning on a-C:H-1 on PEEK. This allows the effusion of interstitial embedded hydrogen within the coating to the toplayer and initiates a passivation by terminating still unbonded free carbon bindings. Through this, an increased number of hydrogen-terminated carbon bonds are built and aligned with the surface or contour of the counterpart through tribological contact. Erdemir [34] showed that the hydrogen is able to create dipoles that keep electrons away from the surface. As the proton takes the electrons place, interactions with other lubricant or counterpart molecules are prevented. Moreover, C–H bindings are covalent and stronger compared to a single C–C bonding, allowing the C–H bonds to withstand even increased loads. In addition, even if a C–H bond would break in consequence of the tribological load, the rearrangement by topological disorder could enable the release of interstitial embedded hydrogen with the possibility to replenish the open binding. Thereby, the coating structure acts as a reservoir.

In case of the a-C:H-2 on PA66 coating under slow conditioning, the effect of the described mechanism is smaller. A reason could be the basic molecular structure differs from the a-C:H-1 on PEEK coatings as well as properties like the indentation hardness H_{IT} and modulus of indentation E_{IT} as shown in [22].

5 Conclusions

The influence of DLC on the tribological behavior of PEEK and PA66 in highly stressed rolling-sliding contacts is considered using a twin-disk tribometer. Additional, SEM and Raman analysis enable a deeper understanding of the molecular changes within the DLC coatings and the effects on friction. The results can be concluded as follows:

- The coatings show sufficient adhesion even under harsh rolling-sliding conditions.
- Wear is reduced by the application of a-C:H on PEEK and PA66 compared to uncoated polymers.
- Friction in mixed lubrication with mineral oil is affected by the coating and initial conditioning process.
- The coatings show hardly any influence on the friction and temperature behavior at fluid-film lubrication.

- The topological disorder of a-C:H has a significant effect on the coefficient of friction in mixed lubrication.

In the future, further tribological analyses are planned. The goal is to transfer the gained knowledge on DLC coatings on polymers and the tribological behavior to polymer spur gears and to enable a higher load-carrying capacity compared to uncoated gears.

Acknowledgements The presented results are based on the research project BO 1979/57-1 and STA 1198/15-1 within the collaborative research with BUT and IOT; supported by the German Research Foundation e.V. (DFG)/Bavarian Research Foundation (BFS) in cooperation with Czech Science Foundation (GACR) 18-26849J. The authors would like to thank for the sponsorship and support received from the DFG/BFS and GACR. The authors would like to thank the Evonik Resource Efficiency GmbH (Kirschenallee; D-64293 Darmstadt) and the Teknor Germany GmbH (Am Rödlein 1; D-91541 Rothenburg ob der Tauber) for providing the raw material for the specimens. We also thank Klüber Lubrication München SE&Co. KG (Geisenhausenerstraße 7; D-81379 München) for providing the lubricants.

Author Contributions KS, TL, EM, SR, KB, CK, MT, PŠ, MH: Conceptualization; Methodology. KS, KB, MH: Resources. KS, TL, EM, KB, CK, MH: Writing–Review & Editing; Funding acquisition. KS, TL, KB, CK, MH: Supervision; Project administration. EM, SR, MT, PŠ; Investigation. SR, MT: Writing–Original Draft. PŠ: Writing – Contribution to Original Draft. SR, MT, PŠ: Visualization.

Funding Open Access funding enabled and organized by Projekt DEAL. This study was funded by German Research Foundation, Deutsche Forschungsgemeinschaft (DFG), within the project within the project “Thermo-Elastohydrodynamics of Coated Polymer Gears” BO 1979/57–1 and STA 1198/8–1 in cooperation with Czech Science Foundation (GACR) 18-26849 J.

Data Availability The data that support the findings of this study are available from the corresponding author upon reasonable request.

Declarations

Conflict of Interest The authors declare that they have not known competing financial interests or personal relationships that could have appeared to influence the work reported in this paper.

Code availability Not applicable.

Open Access This article is licensed under a Creative Commons Attribution 4.0 International License, which permits use, sharing, adaptation, distribution and reproduction in any medium or format, as long as you give appropriate credit to the original author(s) and the source, provide a link to the Creative Commons licence, and indicate if changes were made. The images or other third party material in this article are included in the article's Creative Commons licence, unless indicated otherwise in a credit line to the material. If material is not included in the article's Creative Commons licence and your intended use is not permitted by statutory regulation or exceeds the permitted use, you will need to obtain permission directly from the copyright holder. To view a copy of this licence, visit <http://creativecommons.org/licenses/by/4.0/>.

References

- Erhard, G.: *Konstruieren mit Kunststoffen*. Carl Hanser Verlag, München, Wien (2004)
- Ehrenstein, G.W.: *Mit Kunststoffen konstruieren*. Carl Hanser Verlag, Eine Einführung. München (2007)
- Fürstenberger, M.: *Betriebsverhalten verlustoptimierter Kunststoffzahnräder*. Technische Universität München Dissertation, München (2013)
- Hasl, C., Illenberger, C., Stahl, K., Tobie, T.U., Oster, P.: Potential of oil-lubricated cylindrical plastic gears. *J. Adv. Mech. Design Syst. Manuf.* **12**(1), S. 1-9 (2018)
- Bartel, D.: *Simulation von Tribosystemen: Grundlagen und Anwendungen*. Vieweg+Teubner, Wiesbaden (2010)
- Vincente, J.D., Stokes, J.R.U., Spikes, H.A.: The frictional properties of Newtonian fluids in rolling-sliding soft-EHL contact. *Tribol. Lett.* **20**(3–4), S. 273–286 (2005)
- Ziegltrum, A., Maier, E., Lohner, T.U., Stahl, K.: A numerical study on thermal elastohydrodynamic lubrication of coated polymers. *Tribol. Lett.* **68**, 71 (2020)
- Reitschuster, S., Maier, E., Lohner, T.U., Stahl, K.: Friction and temperature behavior of lubricated thermoplastic polymer contacts. *Lubricants* **8**, 67 (2020)
- Maier, E., Ziegltrum, A., Lohner, T.U., Stahl, K.: Characterization of TEHL contacts of thermoplastic gears. *Forsch. Ingenieurwes.* **81**, S. 317–324 (2017)
- Kano, M.: *Overview of DLC-coated engine components*. Springer International Publishing (2015)
- Lugscheider, E., Bobzin, K., Maes, M.U., Krämer, A.: On the coating of polymers—basic investigations. *Thin Solid Films* **459**, 313–317 (2004)
- Martinez-Martinez, D.U., de Hosson, J.T.M.: On the deposition and properties of DLC protective coatings on elastomers: a critical review. *Surface Coat. Technol.* **258**, 677–690 (2014)
- Rothammer, B., Marian, M., Neusser, K., Bartz, M., Böhm, T., Krauß, S., Schroeder, S., Uhler, M., Thiele, S., Merle, B., Kretzler, J.P.U., Wartzack, S.: Amorphous carbon coatings for total knee replacements—Part II: tribological behavior. *Polymers* **13**, 1880 (2021)
- Puertolas, J.A., Martinez-Nogues, V., Martinez-Morlanes, M.J., Mariscal, M.D., Medel, F.J., Lopez-Santos, C.U., Yubero, F.: Improved wear performance of ultra high molecular weight polyethylene coated with hydrogenated diamond like carbon. *Wear* **269**(5–6), 458–465 (2010)
- Onate, J.I., Comin, M., Bracerias, I., Garcia, A., Viviente, J.L., Bri-zuela, M., Garagorri, N., Peris, J.L.U., Alava, J.I.: Wear reduction effect on ultra-high-molecular-weight polyethylene by application of hard coatings and ion implantation on cobalt chromium alloy, as measured in a knee wear simulation machine. *Surface Coat. Technol.* **142–144**, 1056–1062 (2001)
- Kaczorowski, W., Szymanski, W., Batory, D.U., Niedzielski, P.: Tribological properties and characterization of diamond like carbon coatings deposited by MW/RF and RF plasma-enhanced CVD method on poly(ether-ether-ketone). *Plasma Process Polym.* **11**, 878–887 (2014)
- Bobzin, K., Brögelmann, T., Kalscheuer, C. u. Thiex, M.: Steigerung der Leistungsfähigkeit technischer Kunststoffe durch DLC-Beschichtungen. *Tribologie und Schmierungstechnik* **67** (2020)
- Elsharkaxy, A.A., Holmes, M.J.A., Evans, H.P., Snidle, R.W.: Micro-elastohydrodynamic lubrication of coated cylinders using coupled differential deflection method. *Proc. Inst. Mech. Eng.* **220**, 29–41 (2006)
- Kalish, R., Lifshitz, Y., Nugent, K., Prawer, S.: Thermal stability and relaxation in diamond-like-carbon: a Raman study of films with different sp³ fractions (ta-C to a-C). *Appl. Phys. Lett.* **74**, 2936–2938 (1998)
- Ferrari, A.C., Robertson, J.: Interpretation of Raman spectra of disordered and amorphous carbon. *Phys. Rev. B* **61**, 14095–14107 (2000)
- Casiraghi, C., Ferrari, A.C., Robertson, J.: Raman spectroscopy of hydrogenated amorphous carbons. *Phys. Rev. B* (2005). <https://doi.org/10.1103/PhysRevB.72.085401>
- Bobzin, K., Kalscheuer, C., Thiex, M., Sperka, P., Hartl, M., Reitschuster, S., Maier, E., Lohner, T., Stahl, K.: DLC Coated thermoplastics: tribological analyses under dry and lubricated sliding conditions. Status: Submitted Simultaneously to Tribology Letters (2022)
- Norm DIN EN ISO 4288:1998. Geometrical Product Specifications (GPS)—surface texture: profile method—rules and procedures for the assessment of surface texture
- Laukotka, E.M.: *Referenzöle Datensammlung*. FVA-Heft Nr. 660 Forschungsvereinigung Antriebstechnik e.V. (2007)
- Myers, T.G., Hall, R.W., Savage, M.D., Gaskell, P.H.: The transition region of elastohydrodynamic lubrication. *Proc. Math. Phys. Sci.* **432**(1886), S469-479 (1991)
- Niemann, G., Winter H.: *Maschinenelemente Band 2: Getriebe allgemein, Zahnradgetriebe—Grundlagen, Stirnradgetriebe*. Berlin, Heidelberg: Springer-Verlag (2003)
- Bobzin, K., Brögelmann, T., Kalscheuer, C., Thiex, M., Ebner, M., Lohner, T., Stahl, K.: A contribution to the thermal effects of DLC coatings on fluid friction in EHL contacts. *Lubrication Sci.* **30**, S285-299 (2018)
- Chen, Z., Liu, Y., Zhang, S., Luo, J.: Superlubricity achieved with mixtures of polyhydroxy alcohols and acids. *Langmuir* **29**, 5239–5245 (2013)
- Wang, H., Liu, Y., Li, J., Luo, J.: Investigation of superlubricity achieved by polyalkylene glycol aqueous solutions. *Adv Mater Interfaces* **3**, 1600531 (2016)
- Yilmaz, M., Lohner, T., Michaelis, K., Stahl, K.: Minimizing gear friction with water-containing gear fluids. *Forsch Ingenieurwes* **83**, S327-337 (2019)
- Lohner, T., Mayer, J., Michaelis, K., Höhn, B.-R., Stahl, K.: On the running-in behavior of lubricated line contacts. *Proc. Inst. Mech. Eng.* **231**, 441–452 (2017)
- Bobzin, K., Brögelmann, T., Kalscheuer, C., Thiex, M., Stahl, K., Lohner, T., Maier, E., Reitschuster, S.: Steigerung der Leistungsfähigkeit technischer Kunststoffe durch DLC-Beschichtungen. *Proceeding of the 60th German Tribology Conference (GfT) Göttingen* (2019)
- Ferrari, A. C., Robertson, J.: Resonant Raman spectroscopy of disordered, amorphous, and diamondlike carbon. *Phys. Rev. B* **64** (2001)
- Erdemir, A.: Design Criteria for Superlubricity in Carbon Films and Related Microstructures. *Tribology International* **37**, 577–583 (2004)
- Computer Aided Material Preselection by Uniform Standards CAMPUS: CAMPUS—a material information system for the plastics industry Computer Aided Material Preselection by Uniform Standards. <https://www.campusplastics.com/>
- Martienssen, W., Warlimont, H.: *Handbook of condensed matter and materials data*. Springer-Verlag, Berlin, Heidelberg (2005)

Publisher's Note Springer Nature remains neutral with regard to jurisdictional claims in published maps and institutional affiliations.